Int. J. Heat Mass Transfer. Vol. 19, pp. 827–838. Pergamon Press 1976. Printed in Great Britain

FREE CONVECTION MASS TRANSFER FROM HORIZONTAL PLATES

J. BANDROWSKI and W. RYBSKI
Silesian Technical University, Institute of Chemical Engineering and Chemical Apparatus Construction, Gliwice, Poland

(*Received* 18 *December* 1974)

Abstract—Process of free-convection mass transfer from horizontal plates has been analysed theoretically. For two opposite orientations of active surface of semi-infinite strip delivering the mass downwards, viz. upward position and the downward one, the corresponding easily applicable correlation equations, in dependence on two characteristic parameters: Sc, Schmidt number and y_{A_0}, initial concentration on the plate, have been obtained. In the case of the upward orientation of the active surface the solution has been carried out by making use of the integral treatment, whereas for the downward orientation of active surface the similarity solution has been used. The results obtained for both characteristic cases studied are very close to each other. The comparison with the experimental data available shows a quite good agreement.

NOMENCLATURE

A, constant defined by equation (29);
a, half of plate length;
C, molar concentration;
D, kinematic diffusivity;
F, function defined by equation (44);
Gr_m, Grashof number defined by equation (16);
g, acceleration due to gravity;
M, molecular mass;
P, pressure;
P', pressure defined by equations (5) and (39);
P_0, constant;
Ra_m, modified Rayleigh number $= (Gr_m Sc)$;
Sc, Schmidt number $= \nu/D_A$;
Sh, Sherwood number $= \beta_A a/D_A C$;
u, independent variable defined by equation (31);
u_x, velocity component in the direction of x axis;
y, mole fraction;
y_1, independent variable defined by equation (22).

Greek symbols

α, quantity defined by equation (8);
β, mass-transfer coefficient;
δ, thickness of boundary layer;
η, independent variable in equations (13), (14) and (45);
ϑ, velocity component in the direction of y axis;
ν, kinematic viscosity;
ρ, density;
ϕ, function defined by equation (44);
ψ, stream function.

Subscripts

A, refers to the diffusing component;
0, refers to the plate surface;
∞, refers to the medium.

The horizontal bar over the individual symbols denotes dimensionless quantities.

1. INTRODUCTION

THE FREE convection mass transfer from horizontal plates has been hitherto the subject of only few experimental works. One of the earliest contributions to this problem was the study made by Wragg [1]. Natural convection mass-transfer phenomena were investigated by making use of the electrochemical technique. The mass-transfer coefficient was determined by measurements of limiting currents for the deposition of copper on copper electrodes from acidified cupric sulphate solutions. The correlation equations for the mean Sherwood number, in dependence on modified Rayleigh number $Ra_m = Sc \cdot Gr_m$, were as follows:

$$Sh = 0.64\,(Ra_m)^{0.25} \quad \text{for} \quad 10^4 \leqslant Ra_m \leqslant 2.5 \times 10^7$$
$$Sh = 0.16\,(Ra_m)^{0.33} \quad \text{for} \quad 2.5 \times 10^7 \leqslant Ra_m \leqslant 10^{12}$$

Wragg and Loomba [2], using the improved experimental apparatus, have extended the previous research [1]. The data obtained were correlated by the equations:

$$Sh = 0.75\,(Ra_m)^{0.25} \quad \text{for} \quad 3 \times 10^4 \leqslant Ra_m \leqslant 3 \times 10^7$$

and

$$Sh = 0.18\,(Ra_m)^{0.33} \quad \text{for} \quad 3 \times 10^7 \leqslant Ra_m \leqslant 10^{12}.$$

Similar results, obtained by the same electrochemical technique, are presented in the work of Fenech and Tobias [3]. For high values of the product $Sc \cdot Gr_m$, ranging from 10^8 to 1.4×10^{12}, the mean Sherwood number was given by the relationship: $Sh = 0.19\,(Sc\,Gr_m)^{1/3}$. All the works mentioned above refer to the case of horizontal plates with active surface facing upwards and delivering the mass in the same direction.

Bandrowski *et al.* [4, 5] made an attempt of comparing the experimental results for horizontal plates with active surface directed upwards and downwards. Carrying out the studies on free convection mass transfer from rectangular horizontal plates covered

with naphthalene, the authors have presented the following correlation equations:

(i) for a plate facing downwards and delivering the mass downwards:

$$Sh = 0.69\,(Sc\,Gr_m)^{0.222} \tag{4}$$

(ii) for a plate facing upwards and delivering the mass downwards:

$$Sh = 1.27\,(Sc\,Gr_m)^{0.169}. \tag{5}$$

The values of the product $Sc \cdot Gr_m$ in both cases ranged from 3×10^3 to 2.5×10^5.

Recently Goldstein *et al.* [6] performed the experiments on natural convection mass transfer adjacent to horizontal plane surface, using the naphthalene sublimation technique. For the studied case of plates with active surface facing downwards and delivering the mass downwards, three geometries, viz. circular, square and rectangular plates were employed in the tests. A common correlation for all these planforms was obtained owing to the use of characteristic lengths equal to the ratio of the surface area to the perimeter.

The corresponding correlation equations are:

$$Sh = 0.59\,(Ra_m)^{1/4} \quad \text{for} \quad Ra_m > 200$$

$$Sh = 0.96\,(Ra_m)^{1/6} \quad \text{for} \quad Ra_m < 200.*$$

The aim of the present paper is to solve the mentioned problem theoretically. The whole work will be divided into two parts, viz.: (i) free convection mass transfer from horizontal plates with active surface facing upwards and delivering the mass downwards, and (ii) free convection mass transfer from horizontal plates with active surface facing downwards and delivering the mass downwards.

2. THE SOLUTION FOR THE UPWARD-FACING PLATES

In this case the concentration-induced density differences give rise to buoyancy forces which produce natural convection motion initiated in the plate centre and continued towards plated edges. The generated boundary-layer thickness reaches its maximum at the plate centre and decreases along the plate to achieve the minimum value at the edges. Taking into account the coordinate system shown in Fig. 1 and assuming the boundary-layer approximation, the steady-state momentum-, continuity-, and diffusion-equations can be written as follows:

$$u\frac{\partial u}{\partial x} + \vartheta\frac{\partial u}{\partial y} = \frac{1}{\rho}\frac{\partial P'}{\partial x} + \nu\frac{\partial^2 u}{\partial y^2} \tag{1}$$

$$0 = -\frac{\partial P'}{\partial y} - g(\rho - \rho_\infty) \tag{2}$$

$$\frac{\partial u}{\partial x} + \frac{\partial \vartheta}{\partial y} = 0 \tag{3}$$

$$u\frac{\partial y_A}{\partial x} + \vartheta\frac{\partial y_A}{\partial y} = D_A\frac{\partial^2 y_A}{\partial y^2} \tag{4}$$

*After sending the manuscript of this work to the Editor, Lloyd and Moran [11] published a paper, being the result of mass-transfer studies (carried out by means of an electrochemical method) for horizontal plates with the active surface facing upwards. The obtained relationship in the form $Sh = 0.54 \times Ra_m^{1/5}$ for $2.2 \times 10^4 \leqslant Ra_m \leqslant 8 \times 10^6$ is very close to the equation of Goldstein *et al.* [6].

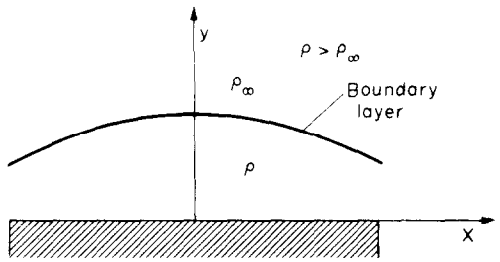

FIG. 1. Scheme of the boundary layer.

where

$$P' = P + g\rho_\infty y + P_0. \tag{5}$$

The corresponding boundary conditions are

$$y = 0;\ u = 0,\ \vartheta = \vartheta_0,\ \frac{\partial u}{\partial y} = \left(\frac{\partial u}{\partial y}\right)_0,\ y_A = y_{A_0} \tag{6}$$

$$y \to \infty;\ u \to \vartheta \to 0,\ \frac{\partial u}{\partial y} \to 0,\ y_A \to 0,\ \frac{\partial y_A}{\partial y} \to 0. \tag{7}$$

Density differences in equation (2) can be expressed as

$$\rho - \rho_\infty = y_A\frac{M_A - M_B}{M} = y_A\alpha. \tag{8}$$

Substituting P', which is obtained by integrating (2) from y to δ with respect to y, into (1), and regarding (8), we obtain

$$u\frac{\partial u}{\partial x} + \vartheta\frac{\partial u}{\partial y} = -g\alpha\frac{\partial}{\partial x}\int_y^\delta y_A\,\mathrm{d}y + \nu\frac{\partial^2 u}{\partial y^2}. \tag{9}$$

Adding (9) to (3), integrating from 0 to δ with respect to y and allowing for the boundary conditions (6) and (7), we get

$$\frac{\partial}{\partial x}\int_0^\delta u^2\,\mathrm{d}y = -g\alpha\frac{\partial}{\partial x}\int_0^\delta \mathrm{d}y\int_y^\delta y_A\,\mathrm{d}y - \nu\left(\frac{\partial u}{\partial y}\right)_0. \tag{10}$$

Proceeding in the same way with (4), we can finally write

$$\frac{\partial}{\partial x}\int_0^\delta (u \cdot y_A)\,\mathrm{d}y - y_{A_0}\vartheta_0 = -D_A\left(\frac{\partial y_A}{\partial y}\right)_0 \tag{11}$$

where

$$\vartheta_0 = -\frac{D_A}{1 - y_{A_0}}\left(\frac{\mathrm{d}y_A}{\mathrm{d}y}\right)_0. \tag{12}$$

After assumption of velocity and concentration profiles given by Eckert [7]

$$u = u_x\eta(1-\eta)^2 \tag{13}$$

$$y_A = y_{A_0}(1-\eta)^2 \tag{14}$$

and introduction of dimensionless variables

$$\bar{x} = \frac{x}{a},\quad \bar{u}_x = u_x a(Gr_m Sc)^{-2/5}\frac{1}{D_A},$$

$$\bar{\delta} = \delta(Gr_m Sc)^{1/5}\frac{1}{a} \tag{15}$$

where

$$Gr_m = y_A g\alpha a^3/\nu^2 \tag{16}$$

equations (10) and (11) reduce to

$$\tfrac{1}{105}\frac{1}{Sc}\frac{\mathrm{d}}{\mathrm{d}\bar{x}}(\bar{u}_x^2\bar{\delta}) = -\tfrac{1}{12}\frac{\mathrm{d}\bar{\delta}^2}{\mathrm{d}\bar{x}} - \frac{\bar{u}_x}{\bar{\delta}} \tag{17}$$

$$\frac{\mathrm{d}}{\mathrm{d}\bar{x}}(\bar{u}_x\bar{\delta}) = \frac{60}{1 - y_{A_0}}\frac{1}{\bar{\delta}}. \tag{18}$$

The above equations are first-order, non-linear differential equations. Thus, their solution requires two boundary conditions. One of them is determined by symmetry at $\bar{x} = 0$, i.e. where the flow begins, which explicitly means that velocity at the plate centre must be zero.

$$\bar{u}_x(0) = 0. \tag{19}$$

The second boundary condition involves the boundary-layer depth at the plate edge.

Following the method described by Clifton and Chapman [8], the use was made of the analogy between the boundary-layer flow and the flow in open channels. Assuming the minimum boundary-layer depth at the plate edge obtained by application of the minimum allowable energy of flowing stream (details of derivation can be found in [8]), for dimensionless plate length $\bar{x}$ at plate edge (e.g. when $\bar{x} = 1$) the boundary-layer thickness can be expressed as:

$$\bar{\delta}(1) = \left[\frac{540}{(1-y_{A_0})^2\, Sc}\left(\int_0^1 \frac{d\bar{x}}{\bar{\delta}}\right)^2\right]^{1/3}. \tag{20}$$

Thus, (20) is the second boundary condition for equations (17) and (18) to be solved. The mean Sherwood number based on the plate half-length a, has the form

$$Sh = \frac{\beta_A \cdot a}{D_A \cdot C} = 2(Gr_m\, Sc)^{1/5} \int_0^1 \frac{d\bar{x}}{\bar{\delta}}. \tag{21}$$

As can be seen from (21), the determination of mass-transfer coefficient requires the knowledge of the variation of boundary layer thickness along the plate length: $\bar{\delta} = \bar{\delta}(\bar{x})$.

Proceeding to the solution of (17) and (18), let us introduce a new independent variable:

$$y_1 = \bar{u}_x \cdot \bar{\delta} \tag{22}$$

Equations (17) and (18) become

$$\frac{d\bar{\delta}}{dx} = 6\left(\frac{120}{1-y_{A_0}} + 105\, Sc\right)\frac{y_1}{6y_1^2 - 105\, Sc\, \bar{\delta}^3} \tag{23}$$

$$\frac{dy_1}{d\bar{x}} = \frac{60}{\bar{\delta}(1-y_{A_0})} \tag{24}$$

with the boundary conditions

$$y_1(0) = 0 \tag{25}$$

$$\bar{\delta}(1) = \left(\frac{3}{20\, Sc}\right)^{1/3} [y_1(1)]^{2/3}. \tag{26}$$

The last condition results from substitution of integral form of equations (19)–(20). When the Lagrange method of solving differential equations is employed to just-derived boundary problem, we can write

$$y_1^2 = \frac{105\, A\, Sc}{6(3-A)}[\bar{\delta}(0)]^3\left\{\left[\frac{\bar{\delta}}{\bar{\delta}(0)}\right]^A - \left[\frac{\bar{\delta}}{\bar{\delta}(0)}\right]^3\right\} \tag{27}$$

$$\bar{u}_x^2 = \frac{105\, A\, Sc}{6(3-A)}\{[\bar{\delta}(0)]^{3-A} \cdot \bar{\delta}^{A-2} - \bar{\delta}\} \tag{28}$$

where

$$A = \frac{120}{120 + 105\, Sc\,(1-y_{A_0})}. \tag{29}$$

In order to find the unknown function $\bar{\delta} = \bar{\delta}(\bar{x})$, equations (27) and (23) can be combined to yield

$$\frac{d\bar{\delta}}{d\bar{x}} = 6\left(\frac{120}{1-y_{A_0}} + 105\, Sc\right) \times \frac{\sqrt{\left(\frac{105\, Sc\, A}{6(3-A)}[\bar{\delta}(0)]^3\right)} \cdot \sqrt{\left(\left[\frac{\bar{\delta}}{\bar{\delta}(0)}\right]^A - \left[\frac{\bar{\delta}}{\bar{\delta}(0)}\right]^3\right)}}{\frac{105\, Sc\, A}{(3-A)}[\bar{\delta}(0)]^3\left\{\left[\frac{\bar{\delta}}{\bar{\delta}(0)}\right]^A - \left[\frac{\bar{\delta}}{\bar{\delta}(0)}\right]^3\right\} - 105\, Sc\, \bar{\delta}^3}. \tag{30}$$

Let us introduce a new independent variable

$$\sin^2 t = \left[\frac{\bar{\delta}(\bar{x})}{\bar{\delta}(0)}\right]^{3-A} = U^{3-A}. \tag{31}$$

The corresponding boundary conditions have now the form

$$U(0) = 1 \tag{32}$$

$$U(1) = \left(\frac{21\, A}{24 + 13\, A}\right)^{1/(3-A)}. \tag{33}$$

Separating the variables in (30), after substituting (31) and integrating from U (1) to U (0) with respect to U, we have

$$\bar{x} = 1 - \frac{\displaystyle\int_{\sin^{-1}\left[\left(\frac{21A}{24+13A}\right)^{1/2}\right]}^{\sin^{-1}[U^{(3-A)/2}]} \left(-\frac{A}{3} + \sin^2 t\right)\sin^{(2A-1)/(3-A)} t\, dt}{\displaystyle\int_{\sin^{-1}\left[\left(\frac{21A}{24+13A}\right)^{1/2}\right]}^{\pi/2} \left(-\frac{A}{3} + \sin^2 t\right)\sin^{(2A-1)/(3-A)} t\, dt} \tag{34}$$

The relationship (34) obtained by means of simplifying substitution (31), is the final solution of problem under consideration. Now, when the integration is performed numerically on the computer, from the value defined by (33), with given step size, to $U = 1$, the profile of boundary layer thickness can be found with any accuracy.

2.1. *Results and conclusions*

The problem of free-convection mass transfer from horizontal plates with active surface facing upwards and delivering the mass downwards has been investigated analytically by approximate integral treatment. The boundary-layer partial differential equations have been transformed to the set of ordinary differential ones, by integrating them across the boundary layer with assumed velocity and concentration profiles. Solution of resulting equations has been performed under the condition of the minimum allowable energy of flowing stream over the plate edge. Introduction of boundary condition at the plate edge, proposed by Clifton and Chapman [8], being the application of open-channel flow to the determination of minimum boundary-layer thickness, allowed to predict the finite boundary-layer depth at the plate edge. This minimum thickness formula seems to be the truest reflection of physical realities of the problem discussed; it enables a thorough study of velocity and concentration fields over the plate length.

At the same time the often-assumed zero boundary-layer thickness simplification at the edges, widespread in analogous heat-transfer case, is avoided.

From the set of derived equations (17), (18) and boundary conditions (19), (20) it follows that the determination of unknown functions $\bar{u}_x = \bar{u}_x(\bar{x})$ and $\bar{\delta} = \bar{\delta}(\bar{x})$ depends on particular combination of parameters: Schmidt number Sc and initial concentration on the plate y_{A_0}. It should be emphasized that appearing in the mass balance equation. Therefore, allowance for both specified parameters leads to many variants of functions to be sought, the amount of which is equal to the second power of respective heat transfer solutions characterized only by one parameter, viz. Prandtl number.

In this paper all combinations of Sc and y_{A_0}, shown in Table 1, have been taken into account. The figures, based on computer output sheets, do not include all

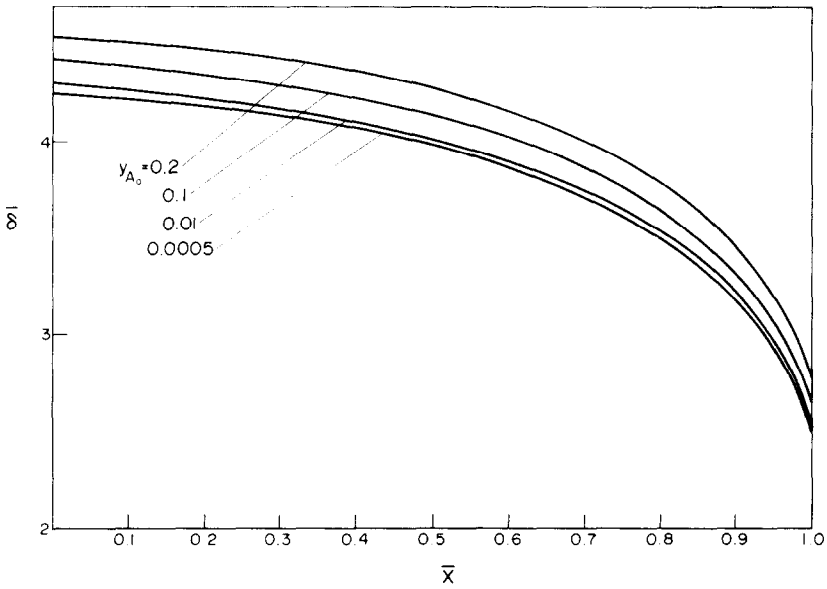

FIG. 2. Thickness of the boundary layer for $Sc = 2.5$.

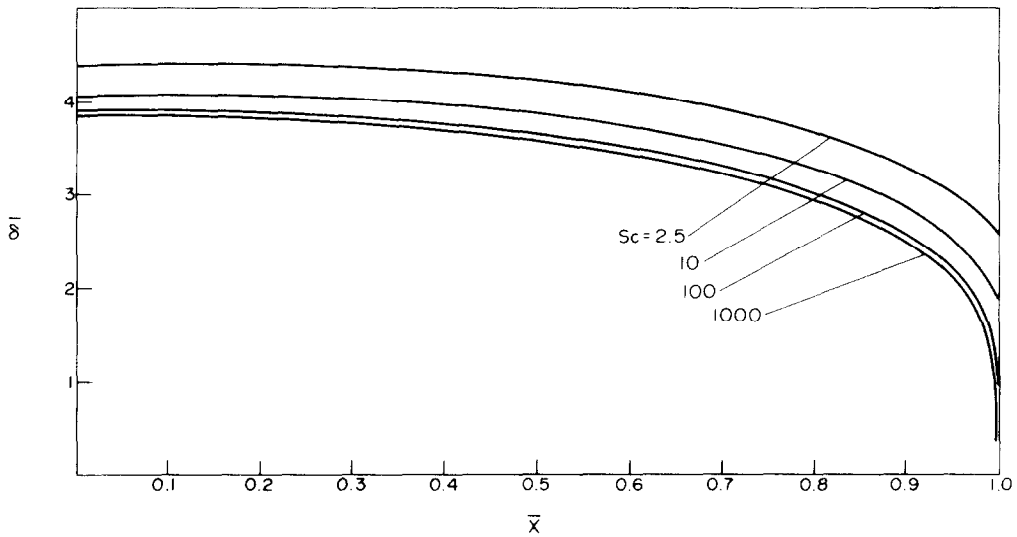

FIG. 3. Thickness of the boundary layer for $y_{A_0} = 0.1$.

the appearance of y_{A_0} parameter is characteristic only for mass transfer and in the radical way distinguishes free-convection mass-transfer equations from corresponding heat-transfer ones. This dissimilarity arises directly from the difference in definition of the boundary conditions on the plate surface in both transfer phenomena. When the heat transfer is considered, the vertical velocity component on the plate surface must be zero, whereas in mass-transfer case there occurs a constant vertical velocity component, obtained solutions, because of similar behaviour of individual solution pairs.

Table 1. Values of the parameters Sc and y_{A_0}

Sc	1	2.5	10	100	1000	2500
y_{A_0}	0.2	0.2	0.2	0.2	0.2	0.2
	0.1	0.1	0.1	0.1	0.1	0.1
	0.01	0.01	0.01	0.01	0.01	0.01
	0.0005	0.0005	0.0005	0.0005	0.0005	0.0005

As a solution pair, full set of results of any row and any column in parameters' Table 1, is understood. So, it may be said that the presented figures are representative in the whole range of parameters Sc and y_{A_0}. The analysis of the obtained results, permits to draw up the following conclusions:

1. Figures 2 and 3 show the dependence of boundary-layer thickness profile on the parameters Sc and y_{A_0}. When the value of Sc is fixed (e.g. 2.5), the rise of the concentration y_{A_0} causes the increase of boundary-layer thickness; on the other hand, when y_{A_0} remains constant, boundary-layer thickness decreases with the Schmidt number increase. Boundary-layer thickness variation is particularly accentuated in the range of small Schmidt numbers at y_{A_0} = const., and in the range of high y_{A_0} values for Sc = const. It can be seen from Fig. 3 that boundary-layer thickness approaches zero at the limit of $Sc \to \infty$.

2. Figures 4 and 5 show the distributions of local Sherwood numbers along dimensionless plate length $\bar{x}$. For Sc being constant the increase of initial concentration y_{A_0} brings about the decrease in Sherwood number values; when y_{A_0} = const. the local Sherwood number increases with the rise of Schmidt number. The high values of Sherwood numbers in the neighbourhood of plate leading edges accentuate the significant influence of finite boundary-layer thickness depth on the mass transfer coefficient.

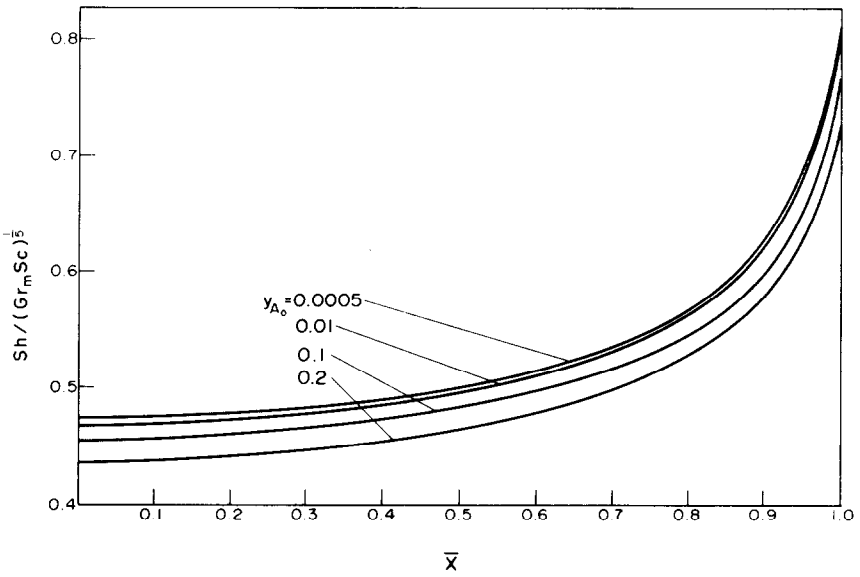

FIG. 4. Variation of the local Sherwood number along the plate length $\bar{x}$ for $Sc = 2.5$.

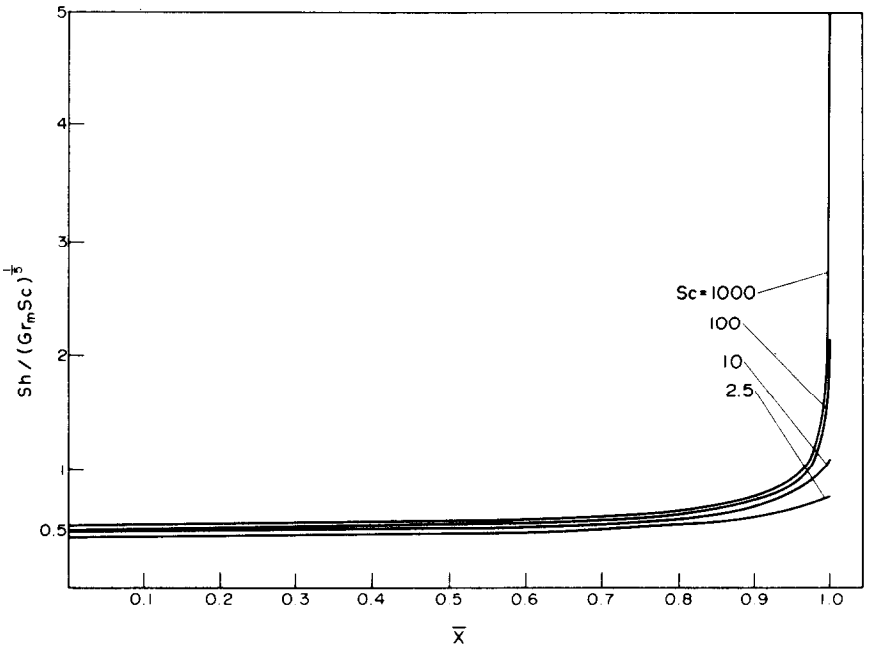

FIG. 5. Variation of the local Sherwood number along the plate length $\bar{x}$ for $y_{A_0} = 0.1$.

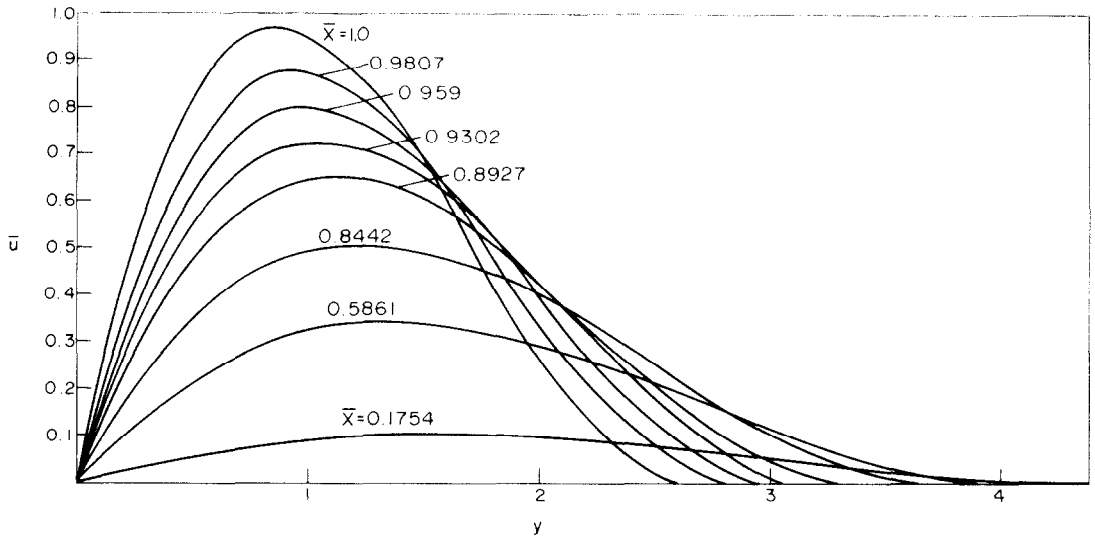

FIG. 6. Velocity profile in the boundary layer for $Sc = 2.5$ and $y_{A_0} = 0.1$.

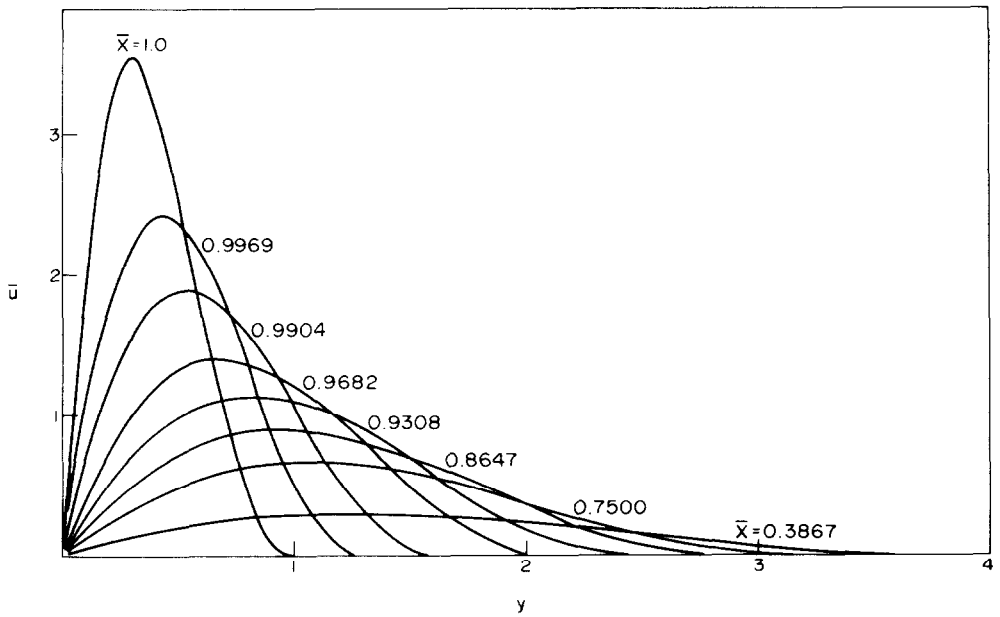

FIG. 7. Velocity profile in the boundary layer for $Sc = 100$ and $y_{A_0} = 0.1$.

3. The velocity distribution in the boundary layer presented in Figs. 6–8, for the exemplary combinations $Sc/y_{A_0} = 2.5/0.1$, 100/0.1 and 100/0.01, shows distinctly the essential effect of plate edges on the velocity profile. It is easy to observe that the main velocity increase appears above the dimensionless plate length $\bar{x} = 0.95$, practically at direct vicinity of leading edges. This fact results from abrupt decrease of boundary-layer thickness above the plate edge, revealed in Figs. 7 and 8 with steep curve slopes near $\bar{x} = 1$. For increasing values of Schmidt number (Figs. 6, 7) the velocity goes up according to boundary layer thickness decrease on the whole plate length. The effect of initial concentration y_{A_0} under condition $Sc = \text{const.}$ is very slight and—as it can be seen from Figs. 7 and 8—the velocity increases to a small extent when the values of y_{A_0} increase. Practically, these variations have such a small order of magnitude that without making any serious error they can be neglected. The above conclusions are valid for all the pairs of solutions.

4. The concentration profile in boundary layer, shown in Figs. 9–11, displays a similar trend as the velocity distribution (cf. above).

Also here, the increase of concentration gradient near the plate edge, in consequence with minimum boundary-layer thickness, was observed. When Schmidt numbers are getting larger, concentration distribution curves become more steep, that means that the reduction of boundary layer thickness causes more violent concentration changes in any arbitrary point of the plate length. Figs. 10 and 11 present concentration profiles for $Sc/y_{A_0} = 100/0.1$ and 100/0.01, respectively. These figures indicate that the decrease of initial concentration y_{A_0} gives occasion to

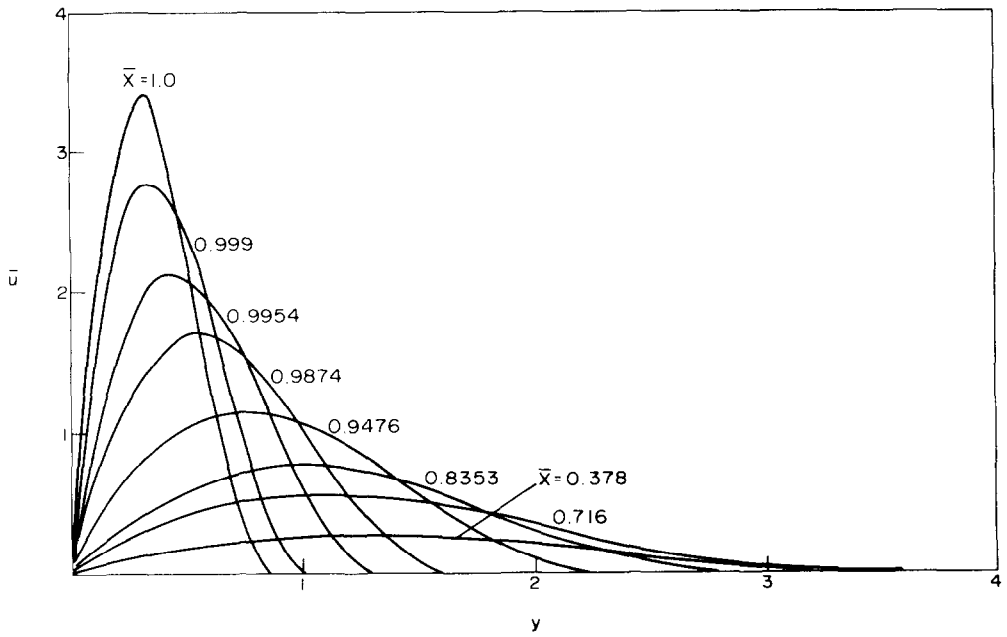

FIG. 8. Velocity profile in the boundary layer for $Sc = 100$ and $y_{A_0} = 0.01$.

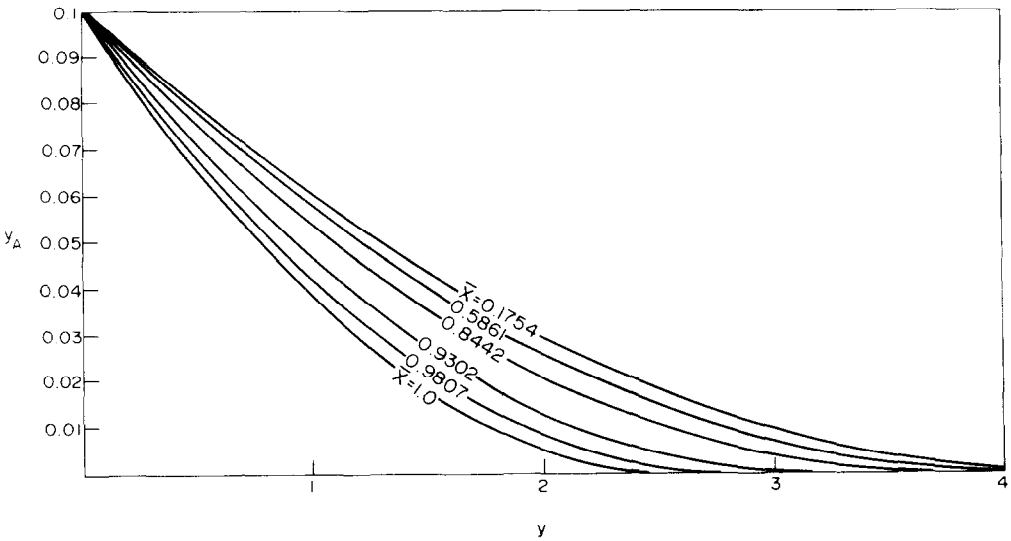

FIG. 9. Variation of the concentration profile in the boundary layer for $Sc = 2.5$ and $y_{A_0} = 0.1$.

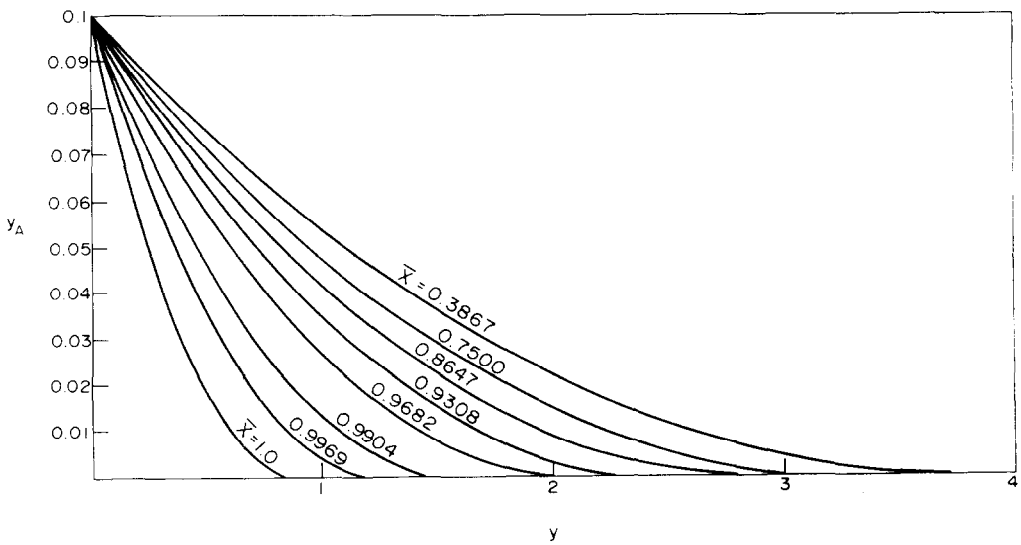

FIG. 10. Variation of the concentration profile in the boundary layer for $Sc = 100$ and $y_{A_0} = 0.1$.

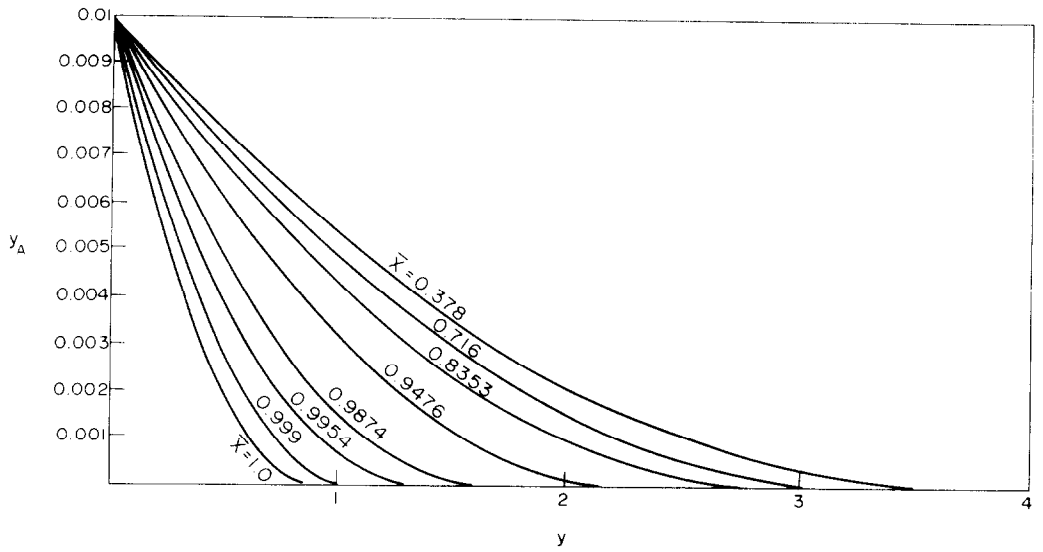

FIG. 11. Variation of the concentration profile in the boundary layer for $Sc = 100$ and $y_{A_0} = 0.01$.

small increase of concentration gradient; practically it seems to be meaningless. The above remarks hold for all obtained pairs of solutions.

5. Both local and average Sherwood numbers are proportional to one-fifth power of modified Rayleigh number; the values of constants appearing in correlation equations, for all pairs of solutions, are given in Table 2. As it can be seen from this table, for constant value of Schmidt number, the average mass-transfer coefficient increases when the initial concentration on the plate y_{A_0} decreases. On the other hand, for any row

Table 2. Values of the constant in the correlation equation for the mean Sherwood number, for individual combinations of parameters Sc and y_{A_0}

y_{A_0}	Sc					
	1	2.5	10	100	1000	2500
0.2	0.4355	0.4925	0.5601	0.5905	0.6024	0.6032
0.1	0.4533	0.5131	0.5744	0.6169	0.6233	0.6236
0.01	0.4687	0.5267	0.5911	0.6242	0.6306	0.6318
0.0005	0.4701	0.5442	0.5917	0.6247	0.6314	0.6327

of Table 2 (y_{A_0} = const.) there is easily visible the recurring tendency of Sherwood number increase with the increase of Schmidt number up to $Sc = 100$, becoming almost constant in the range of $Sc > 100$. The comparison of the results presented above for free-convection mass transfer from horizontal plates facing upwards and general conclusions concerning the analysed mass-transfer phenomena will be made in connection with the results of the opposite variant, viz. when the plate is facing downwards, in the next part of this paper.

3. THE SOLUTION FOR THE DOWNWARD-FACING PLATES

If the plate has the active surface directed downwards and the mass is delivered also downwards, the derivation of the mathematical model is connected not only with the consequence of direction change of buoyancy forces acting, but also with quite different ways of problem analysis. The character of boundary-layer flow initiated at the plate edge and continued towards the plate centre with imposed boundary conditions, establishes a typical example of the possibility of using the similarity solutions method, presented in detail by Hansen [9].

When the previously assumed Boussinesq approximations, concerning density, will be adapted to the present variant of free-convection mass transfer from horizontal plates, schematically shown in Fig. 12, the

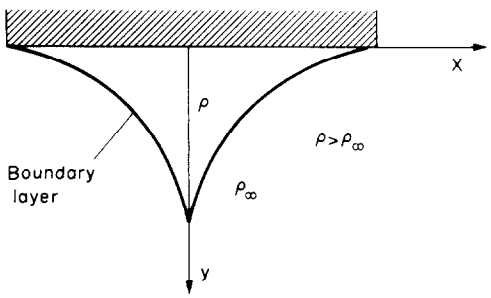

FIG. 12. Scheme of the boundary layer.

governing equations of steady two-dimensional flow become:

$$u\frac{\partial u}{\partial x}+\vartheta\frac{\partial u}{\partial y}=-\frac{1}{\rho}\frac{\partial P'}{\partial x}+\nu\frac{\partial^2 u}{\partial y^2} \tag{35}$$

$$-\frac{\partial P'}{\partial y}+g(\rho-\rho_\infty)=0 \tag{36}$$

$$\frac{\partial u}{\partial x}+\frac{\partial u}{\partial y}=0 \tag{37}$$

$$u\frac{\partial y_A}{\partial x}+\vartheta\frac{\partial y_A}{\partial y}=D_A\frac{\partial^2 y_A}{\partial y^2} \tag{38}$$

where

$$P'=P-g\rho_\infty y+P_0. \tag{39}$$

Equation (35), with allowance for (8), after differentiating with respect to y, can be expressed as:

$$u\frac{\partial^2 u}{\partial x\,\partial y}+\vartheta\frac{\partial^2 u}{\partial y^2}=-g\alpha\frac{\partial y_A}{\partial x}+\vartheta\frac{\partial^3 u}{\partial y^3} \tag{40}$$

The corresponding boundary conditions for (40), (37) and (38), are given by

$$y=0;\quad u=0,\quad \vartheta=\vartheta_0,\quad y=y_{A_0} \tag{41}$$

$$y\to\infty;\quad u\to 0,\quad y_A\to 0,\quad \frac{\partial u}{\partial y}\to 0. \tag{42}$$

Introducing the stream function

$$u=\frac{\partial\psi}{\partial y};\quad \vartheta=-\frac{\partial\psi}{\partial x} \tag{43}$$

and using the following similarity transformation

$$\psi=x^{3/5}F(\eta),\quad y_A=y_{A_0}\phi(\eta) \tag{44}$$

where

$$\eta=yx^{-2/5} \tag{45}$$

the velocity components appearing in equations (37), (38) and (40) can be written:

$$u=x^{1/5}F'(\eta) \tag{46}$$

$$\vartheta=-\tfrac{1}{5}x^{-2/5}[3F(\eta)-2\eta F'(\eta)]. \tag{47}$$

Inserting (46) and (47) into partial differential equations (38) and (40), we obtain a system of ordinary differential equations, which characterizes the discussed mass-transfer case:

$$5\nu F''''+3F'''F+F''F'=-2g\alpha y_{A_0}\phi'\eta \tag{48}$$

$$5D_A\phi''+3F\phi'=0. \tag{49}$$

To avoid dimensional values and, at the same time to get the solution in the form of well-known similarity groups, let us introduce into the above equations the following dimensionless functions:

$$\bar F=\left(Sc^4\frac{\nu^{-3}}{g_x\,y_{A_0}}\right)^{1/5}F,\quad \bar\eta=\left(Sc^{-1}\frac{\nu^2}{g_x\,y_{A_0}}\right)^{-1/5}\eta. \tag{50}$$

Equations (48) and (49) become as follows:

$$5Sc\bar F''''+3\bar F'''\bar F+\bar F''\bar F'=-2Sc\bar\phi'\bar\eta \tag{51}$$

$$5\bar\phi''+3\bar F\bar\phi'=0 \tag{52}$$

The corresponding conditions are: for $\bar\eta=0$

$$\bar\phi(0)=1;\quad \bar F'(0)=0;\quad \bar F(0)=\frac{5}{3}\frac{y_{A_0}}{1-y_{A_0}}\bar\phi'(0) \tag{53}$$

for $\bar\eta\to\infty$

$$\bar\phi(\eta)\to 0;\quad \bar F'(\eta)\to 0;\quad \bar F''(\eta)\to 0. \tag{54}$$

The last condition for $\bar\eta=0$ has an implicit form, resulting from the comparison of relationship (12) with equation (47). The local Sherwood number is obtained from

$$\beta_A\cdot y_{A_0}=-D_AC\left(\frac{dy_A}{dy}\right)_0=-D_ACy_{A_0}\phi'(0)x^{-2/5} \tag{55}$$

which, combined with (50) and integrated along the half-plate length, gives the average Sherwood number over the plate surface, appropriate for examined mass-transfer case.

$$Sh=\frac{\beta_A\cdot a}{D_A\cdot C}=-\tfrac{5}{3}(Gr_m\,Sc)^{1/5}\bar\phi'(0). \tag{56}$$

The solution of (51) and (52) with corresponding boundary conditions (53) and (54) has been carried out numerically.

The method of adjoints used in the present work, is based on the integration of a set of differential equations adjoined with the equations being solved. The details associated with this method can be found in the work of Roberts and Shipman [10].

3.1. *Results and discussion*

The second case of horizontal plate orientation, viz. the active surface facing downwards, has been solved numerically by means of the method of adjoints. The governing equations have been transformed from their initial partial form to the ordinary differential ones by making use of the similarity analysis. Finally, the equations have been reduced to the system of six first-order, non-linear, differential equations and—with the corresponding boundary conditions—were subject to the numerical treatment. The choice of the method of adjoints was inspired by the possibility of using well-known procedures, such as the Runge–Kutta method, or matrix inversion, during its realization on the computer, and by the fact that it converges quadratically, similar to the Newton–Raphson method.

Taking into account that the calculations are time-consuming (e.g. 19 iterations took 3 h or so), the results were obtained only for combinations of Sc and y_{A_0} parameters enclosed in the second column and third row of Table 1. At the same time, the variation of velocity profile $\bar F'$ and concentration $\bar\phi$, shown in Figs. 13 and 14, should be treated as representative of plots for all the combinations of parameters because of small discrepancies between individual values.

The principal results can be summarized as follows:

1. The velocity distribution in the boundary layer has the same character as in the previously studied

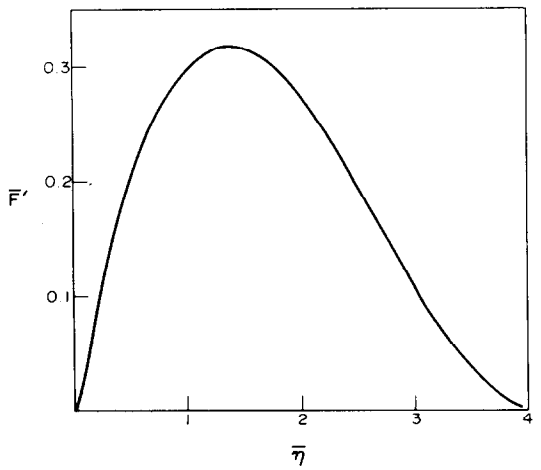

FIG. 13. Velocity profile in the boundary layer for $Sc=100$ and $y_{A_0}=0.01$.

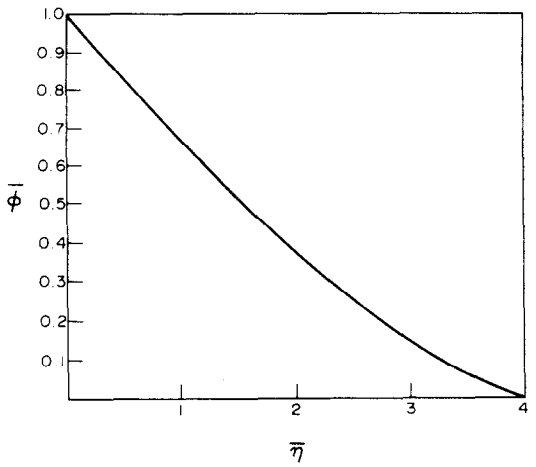

FIG. 14. Concentration profile in the boundary layer for $Sc = 100$ and $y_{A_0} = 0.01$.

first case. Comparing the values of function $\bar{F}'$ given in Table 3, one can see that for increasing Schmidt numbers the velocity slightly decreases. On the other hand, when the values of Schmidt number remain constant, the rise of initial concentration brings about the increase of the velocity, but all these changes are rather small, so the influence of Sc and y_{A_0} parameters on the boundary-layer velocity can be neglected.

coefficient for Schmidt numbers growing up, slightly decreases, becoming almost constant in the range of $Sc > 100$. So, it seems to be quite reasonable to treat the just-discussed mass-transfer problem as independent of the values of Schmidt numbers.

4. COMPARISON OF THEORETICAL AND EXPERIMENTAL RESULTS

Figure 15 shows the lines representative for the experimental results obtained by authors of the papers [2], [4–6], as well as the theoretical data predicted (dashed lines), presented here for two variants of free-convection mass transfer from horizontal plates. In order to compare most adequately the experimental and theoretical results, the theoretically calculated lines have been referred to the parameter set: $Sc = 2.5$ and $y_{A_0} = 0.0005$, since these values are close to the conditions, under which the experiments with sublimating naphthalene have been performed. The great similarity between the experimental results given in [4] and [5] and the theoretical ones, presented in this paper, is very well pronounced.

The agreement of the correlation equations for the upper and lower active surface of horizontal plates, obtained in [4] and [5], corresponds exactly to the almost identical theoretical results for both plate orientation cases.

Table 3

Sc	$\bar{F}'(1)\times 10^2$	$\bar{\phi}(1)\times 10^2$	For $y_{A_0} = 0.01$ $\bar{F}(0)\times 10^4$	$\bar{F}''(0)\times 10^2$	$\bar{F}'''(0)\times 10^2$	$\bar{\phi}'(0)\times 10^2$
1	31.258	66.720	−56.546	52.682	−43.841	−33.588
2.5	30.449	66.874	−56.262	50.522	−41.207	−33.419
10	29.946	66.977	−56.074	49.339	−39.880	−33.308
100	29.785	67.010	−56.014	48.975	−39.484	−33.272
1000	29.769	67.014	−56.008	48.939	−39.445	−33.268
2500	29.767	67.014	−56.007	48.936	−39.442	−33.268

y_{A_0}	$\bar{F}'(1)\times 10^2$	$\bar{\phi}(1)\times 10^2$	For $Sc = 2.5$ $\bar{F}(0)\times 10^4$	$\bar{F}''(0)\times 10^2$	$\bar{F}'''(0)\times 10^2$	$\bar{\phi}'(0)\times 10^2$
0.2	31.445	69.333	−1244.2	51.298	−40.292	−29.862
0.1	30.903	67.979	−588.83	50.885	−40.811	−31.797
0.01	30.449	66.874	−56.262	50.522	−41.207	−33.419
0.0005	30.402	66.758	−2.8005	50.482	−41.244	−33.589

Note: The value $\bar{\eta} = 1$ in the functions $\bar{F}'(\bar{\eta})$ and $\bar{\phi}(\bar{\eta})$ has been chosen arbitrarily for comparison purposes.

2. The concentration variation in the boundary-layer behaves similarly as in the first variant of the plate orientation. From the values of function $\bar{\phi}$, specified in Table 3, it can be seen that when Schmidt number values grow larger, the concentration in the boundary layer slightly increases (concentration gradient decreases); also the increase of y_{A_0} causes the increase of the amount of diffusing component in the boundary layer.

3. Local and average Sherwood numbers are proportional to one-fifth power of the product $Sc \cdot Gr_m$. The values of constant associated with correlation equation increase with y_{A_0} diminishing. When y_{A_0} has a constant value equal to 0.01, the mass-transfer

The lower values of the mass-transfer coefficient calculated theoretically, compared to the experimental data, can be explained by the approximate mathematical model being considered. The restriction of the analysis to the case of two-dimensional flow is directly connected with the disregard of all leading edges, which—as it has been previously pointed out—have a significant effect on the value of mean Sherwood number.

The scantiness of experimental data concerning the free-convection mass-transfer cases discussed, does not allow to perform a more extensive analysis of mass transfer from horizontal plates, so there is a necessity for further experimental research.

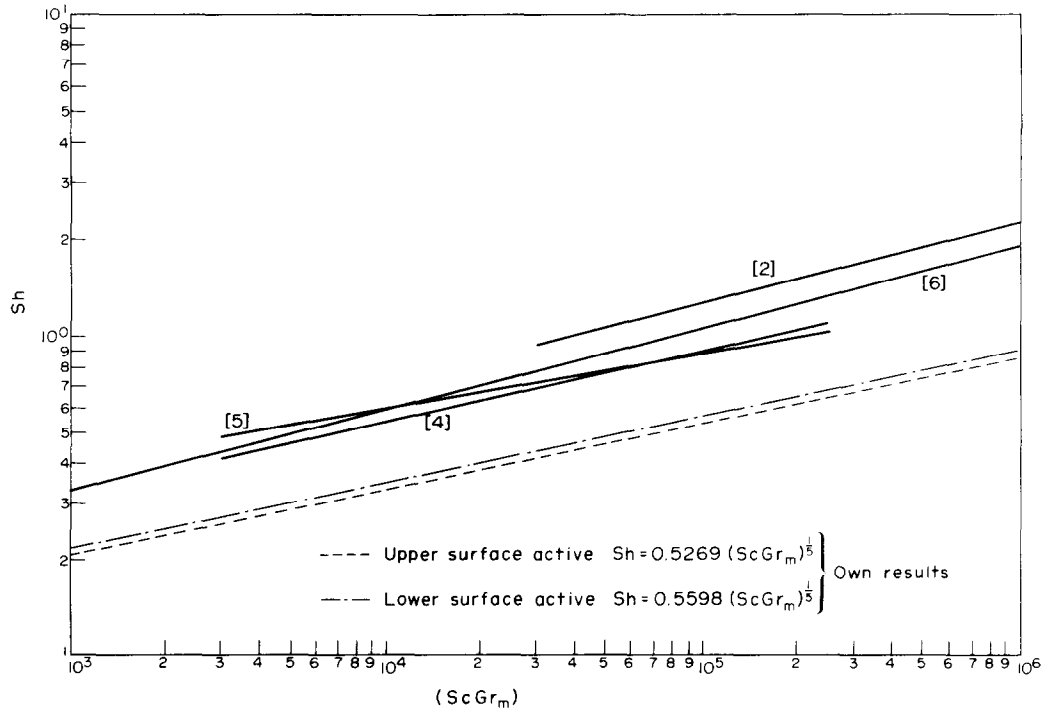

FIG. 15. Comparison of the results for free-convection mass transfer from horizontal plates.

Acknowledgement—The authors are indebted to Dr. Waldemar Krajewski from the Research Centre for Chemical Engineering and Apparatus Construction of Polish Academy of Sciences, Gliwice, for his help in the solution of mathematical problem connected with the first variant of free-convection mass transfer from horizontal plates.

REFERENCES

1. A. A. Wragg, Free convection mass transfer at horizontal electrodes, *Electrochim. Acta* **13**, 2159–2165 (1968).
2. A. A. Wragg and R. P. Loomba, Free convection flow patterns at horizontal surfaces with ionic mass transfer, *Int. J. Heat Mass Transfer* **13**, 439–442 (1970).
3. E. J. Fenech and C. W. Tobias, Mass transfer by free convection at horizontal electrodes, *Electrochim. Acta* **2**, 311–325 (1960).
4. J. Bandrowski, A. Bryczkowski and H. Kominek, Mass transfer in the free flow from a horizontal plate—I. The active surface directed downward and delivering the mass downward (in Polish), *Chemia Stosow.* **6**(4B), 455–464 (1969).
5. J. Bandrowski, A. Bryczkowski and H. Kominek, Mass transfer in the free flow from a horizontal plate—II. The active surface directed upward delivering the mass downward and the surface active on both sides delivering the mass downward (in Polish), *Chemia Stosow.* **7**(2B), 229–240 (1970).
6. R. J. Goldstein, E. M. Sparrow and D. C. Jones, Natural convection mass transfer adjacent to horizontal plates, *Int. J. Heat Mass Transfer* **16**, 1025–1035 (1973).
7. E. R. G. Eckert and R. M. Drake, *Heat and Mass Transfer*, p. 312. McGraw-Hill, New York (1959).
8. J. V. Clifton and A. I. Chapman, Natural convection on a finite size horizontal plate, *Int. J. Heat Mass Transfer* **12**, 1573–1583 (1969).
9. A. G. Hansen, *Similarity Analyses of Boundary Value Problems in Engineering*, p. 9. Prentice-Hall, Englewood Cliffs, NJ (1967).
10. S. M. Roberts and J. S. Shipman, *Two-Point Boundary Value Problems: Shooting Methods*, p. 17. Elsevier, New York (1972).
11. J. R. Lloyd and W. R. Moran, Natural convection adjacent to horizontal surfaces of various planforms, *J. Heat Transfer* **96C**(4), 443–447 (1974).

TRANSFERT MASSIQUE EN CONVECTION NATURELLE SUR DES PLAQUES HORIZONTALES

Résumé—On étudie par voie théorique les processus de transfert de masse en convection libre sur des plaques horizontales. Dans les deux orientations opposées de la surface active de la plaque semi-infinie transférant la masse, c'est à dire orientation vers le haut et vers le bas, on a obtenu les lois de corrélation correspondantes d'application simple qui dépendent de deux paramètres caractéristiques: *Sc* (nombre de Schmidt) et y_{A_0} (concentration initiale sur la plaque). Dans le cas de l'orientation de la surface active vers le haut, la solution a été obtenue par utilisation d'un traitement intégral, tandis que dans le cas d'une orientation dirigée vers le bas la solution en similitude a été utilisée. Les résultats obtenus dans chacun des deux cas caractéristiques étudiés sont très proches l'un de l'autre. La comparaison avec les données expérimentales disponsibles a fourni un très bon accord.

STOFFÜBERGANG VON WAAGERECHTEN PLATTEN BEI FREIER KONVEKTION

Zusammenfassung—Die Stoffübertragung von waagerechten Platten durch freie Konvektion wurde theoretisch analysiert. Für zwei entgegengesetzte Richtungen der massenabgebenden Oberfläche eines halbunendlichen Streifens—aufwärts und abwärts—wurden die Korrelationsbeziehungen in Abhängigkeit

von zwei charakteristischen Parametern, Sc—Schmidt–Zahl und y_{A_0}—Anfangskonzentration an der Oberfläche, erhalten. Für die aufwärtsgerichtete aktive Oberfläche wurde die Lösung aufgrund einer Integralbehandlung erhalten, während für die abwärtsgerichtete aktive Oberfläche eine Ähnlichkeitslösung herangezogen wurde. Die Ergebnisse der beiden untersuchten Fälle sind einander sehr ähnlich. Der Vergleich mit experimentellen Ergebnissen zeigt eine ziemlich gute Übereinstimmung.

ПЕРЕНОС МАССЫ ОТ ГОРИЗОНТАЛЬНЫХ ПЛАСТИН ПРИ СВОБОДНОЙ КОНВЕКЦИИ

Аннотация — Теоретически исследован процесс переноса массы от горизонтальных пластин при свободной конвекции. Для двух противоположных направлений полубесконечной пластины получены соответствующие корреляционные соотношения, представляющие зависимость коэффициента переноса массы от двух характерных параметров: критерия Шмидта, sc, и y_{A0} — начальной концентрации на пластине. В случае активной поверхности, обращенной вверх, решение получено интегральным методом, а для активной поверхности, обращенной вниз, применяется метод подобных решений. Полученные результаты для обоих случаев совпадают очень близко. Сравнение их с имеющимися экспериментальными данными дает довольно хорошее соответствие.